

# Uncovering the Neoproterozoic carbon cycle

D. T. Johnston<sup>1</sup>, F. A. Macdonald<sup>1</sup>, B. C. Gill<sup>1</sup>, P. F. Hoffman<sup>1,2</sup> & D. P. Schrag<sup>1</sup>

Interpretations of major climatic and biological events in Earth history are, in large part, derived from the stable carbon isotope records of carbonate rocks and sedimentary organic matter<sup>1,2</sup>. Neoproterozoic carbonate records contain unusual and large negative isotopic anomalies within long periods (10–100 million years) characterized by  $\delta^{13}\text{C}$  in carbonate ( $\delta^{13}\text{C}_{\text{carb}}$ ) enriched to more than +5 per mil. Classically,  $\delta^{13}\text{C}_{\text{carb}}$  is interpreted as a metric of the relative fraction of carbon buried as organic matter in marine sediments<sup>2–4</sup>, which can be linked to oxygen accumulation through the stoichiometry of primary production<sup>3,5</sup>. If a change in the isotopic composition of marine dissolved inorganic carbon is responsible for these excursions, it is expected that records of  $\delta^{13}\text{C}_{\text{carb}}$  and  $\delta^{13}\text{C}$  in organic carbon ( $\delta^{13}\text{C}_{\text{org}}$ ) will covary, offset by the fractionation imparted by primary production<sup>5</sup>. The documentation of several Neoproterozoic  $\delta^{13}\text{C}_{\text{carb}}$  excursions that are decoupled from  $\delta^{13}\text{C}_{\text{org}}$ , however, indicates that other mechanisms<sup>6–8</sup> may account for these excursions. Here we present  $\delta^{13}\text{C}$  data from Mongolia, northwest Canada and Namibia that capture multiple large-amplitude (over 10 per mil) negative carbon isotope anomalies, and use these data in a new quantitative mixing model to examine the behaviour of the Neoproterozoic carbon cycle. We find that carbonate and organic carbon isotope data from Mongolia and Canada are tightly coupled through multiple  $\delta^{13}\text{C}_{\text{carb}}$  excursions, quantitatively ruling out previously suggested alternative explanations, such as diagenesis<sup>7,8</sup> or the presence and terminal oxidation of a large marine dissolved organic carbon reservoir<sup>6</sup>. Our data from Namibia, which do not record isotopic covariance, can be explained by simple mixing with a detrital flux of organic matter. We thus interpret  $\delta^{13}\text{C}_{\text{carb}}$  anomalies as recording a primary perturbation to the surface carbon cycle. This interpretation requires the revisiting of models linking drastic isotope excursions to deep ocean oxygenation and the opening of environments capable of supporting animals<sup>9–11</sup>.

There are two leading hypotheses for the documented large-amplitude<sup>12</sup> Neoproterozoic carbon isotope anomalies. The first proposal is that the Neoproterozoic deep ocean carried a massive dissolved organic carbon (DOC) reservoir<sup>6</sup>. This model stems from the observation of unlinked changes in  $\delta^{13}\text{C}_{\text{carb}}$  and  $\delta^{13}\text{C}_{\text{org}}$ , with the postulated large DOC pool allowing for  $\delta^{13}\text{C}_{\text{org}}$  records to be buffered against isotopic change. Another view of these large carbon isotopic excursions is represented by a set of hypotheses arguing for the infidelity of  $\delta^{13}\text{C}_{\text{carb}}$  records. In this view, secondary alteration by meteoric waters or burial diagenesis is invoked to satisfy carbon isotope decoupling<sup>7,8</sup>. Given such disparate proposals for explaining the Neoproterozoic carbon isotope record, and the implications for surface environments, climate, oxygen and animals, we aim to revisit the behaviour of the marine carbon cycle and test the validity of the above proposals with a new data set and model.

We sampled stratigraphic sections spanning the mid-Neoproterozoic Cryogenian glacial intermission (<717 to >635 million years ago) at high resolution in Mongolia, northern Namibia and northwest Canada (see Supplementary Information). In Mongolia, limestone of the Tayshir member (of the Tsagaan Oloom Formation) is bracketed by the

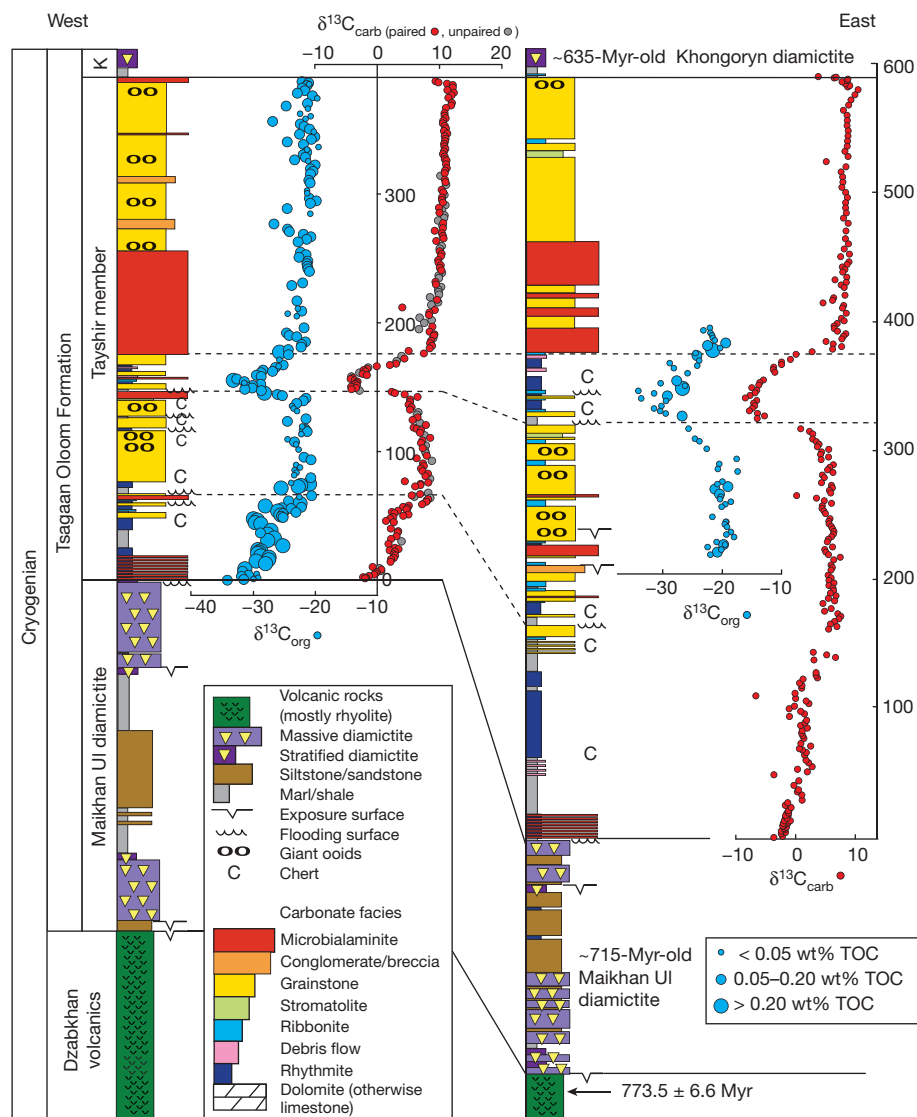
Maikhan Ul and Khongoryn diamictites<sup>13</sup> (Fig. 1). The Tayshir carbon isotope anomaly<sup>13</sup> is recorded in stratigraphic sections throughout the basin, commences with a distinct flooding surface, and is developed predominantly in limestone micrite with relatively low primary porosity. The Tayshir anomaly can either be correlated to moderately negative values in the Gruis Formation of northern Namibia<sup>14</sup> and Bonahaven Dolomite of the British–Irish Caledonides<sup>15</sup>, or to the Trezona anomaly in Australia<sup>16</sup> and Namibia<sup>17,18</sup>. The Trezona anomaly was also sampled through the Ombaatjie Formation in northern Namibia (see Supplementary Information), which directly underlies an erosion surface related to the Ghaub glaciation of  $635.5 \pm 1.2$  million years ago<sup>19</sup>. We further sampled the Cryogenian record from between the glaciations in the Mackenzie Mountains of northwest Canada (see Supplementary Information), where mixed carbonate and siliciclastic rocks of the Twitya and Keele formations are bounded by diamictites of the Sturtian-age Rapitan Group<sup>20</sup> ( $716.47 \pm 0.24$  million years old) and Marinoan-age (~635 million years old) Ice Brook Formation. These strata preserve the post-Sturtian Rasthof anomaly in the Twitya Formation and an anomaly at the top of the Keele Formation that can be correlated to the Trezona anomaly<sup>21</sup>. Although there are alternative published correlations for particular anomalies described above, these correlations are not central to our argument.

We present two  $\delta^{13}\text{C}_{\text{carb}}$  and  $\delta^{13}\text{C}_{\text{org}}$  records through the Tayshir member of Mongolia (Fig. 1). The overall total organic carbon (TOC) contents broadly follow siliciclastic content and are highest at the base of the more distal section (Uliastay Gol), but remain at about 0.08% throughout the succession with no apparent facies dependence (see Supplementary Information). In the Uliastay Gol section ( $n = 171$  pairs), an over 10‰ negative  $\delta^{13}\text{C}_{\text{carb}}$  anomaly (the Tayshir) at a depth of around 150 m preserves an extremely tight coupling with  $\delta^{13}\text{C}_{\text{org}}$  through the entire excursion. Isotopic covariance is observed at even finer stratigraphic scales, such as the inflection recorded at around 50 m depth. Consistent with this, a parallel section 35 km to the east also preserves a tight isotopic coupling and similar net isotopic offset, or  $\epsilon_{\text{TOC}} = \delta^{13}\text{C}_{\text{carb}} - \delta^{13}\text{C}_{\text{org}}$  (Fig. 1; see Supplementary Information).

In northwest Canada, the Cryogenian Twitya and Keele formations provide a comparison to glacial intermission records from Mongolia, and preserve the Rasthof and a latest-Cryogenian isotope excursion (Fig. 2). The post-Sturtian Twitya Formation preserves strong isotopic covariance between carbonate and organic carbon, and an  $\epsilon_{\text{TOC}}$  value that closely approximates what is extracted from Mongolia (see Supplementary Information). The pre-Marinoan Keele Formation also appears to preserve carbon isotope covariance, but records a more variable  $\epsilon_{\text{TOC}}$ , ranging from values similar to those observed in Mongolia to that recorded in the Pleistocene epoch (see Supplementary Information)<sup>5</sup>. In contrast to these records of tight covariance is the Trezona anomaly in Namibia (a TOC-poor dolomudstone, dolograinstone and dolomicrobialaminite; see Supplementary Information), in which  $\delta^{13}\text{C}_{\text{carb}}$  and  $\delta^{13}\text{C}_{\text{org}}$  have little relationship to one another. This later observation is consistent with much of the published Neoproterozoic data<sup>6,10,11,22</sup>. Our data set thus reflects both the convention (isotopic decoupling) as well as strong evidence of isotopic covariance.

<sup>1</sup>Department of Earth and Planetary Sciences, Harvard University, 20 Oxford Street, Cambridge, Massachusetts 02138, USA. <sup>2</sup>School of Earth and Ocean Sciences, University of Victoria, Victoria, British Columbia V8W 2Y2, Canada.

**Figure 1 | Chemostratigraphic sections through the Tayshir member in the Uliastay and Tsagaan Gols (river valleys), Mongolia<sup>13</sup>.** Red and grey symbols represent  $\delta^{13}\text{C}_{\text{carb}}$  data from paired and unpaired samples, respectively (paired  $n = 235$ ). The 2-s.d. errors are smaller than the symbols. The stratigraphic section to the right was measured 35 km to the northeast, a distance shortened by the Cambrian Altaid orogeny<sup>13</sup>. Age constraints on the Dzabkhan volcanics are from ref. 31. K, Khongoryn.



We used these data to evaluate the late-Cryogenian carbon cycle. The classic interpretation of isotopic covariance suggests that biomass is synthesized from a relatively well-mixed marine dissolved inorganic carbon (DIC) reservoir and results in an  $\epsilon_{\text{TOC}}$  value that reflects a kinetic fractionation associated with carbon fixation<sup>2</sup>. This simple depiction of the carbon cycle cleanly explains records from Mongolia and northwest Canada (Figs 1 and 2). Our finding contrasts with models requiring a large DOC pool, which preclude covariance between  $\delta^{13}\text{C}_{\text{carb}}$  and  $\delta^{13}\text{C}_{\text{org}}$ . That is, data from Mongolia and northwest Canada are quantitatively inconsistent with a large DOC model (Figs 1 and 2). It has also been argued that burial diagenesis<sup>8</sup> or meteoric alteration<sup>7</sup> could reset the primary  $\delta^{13}\text{C}_{\text{carb}}$ , calling into question the robustness of carbonate records and their use as a pre-fossil correlation tool. Rather than targeting the fidelity of  $\delta^{13}\text{C}_{\text{org}}$ , these studies emphasize the tight covariance between  $\delta^{13}\text{C}_{\text{carb}}$  and  $\delta^{18}\text{O}_{\text{carb}}$  through certain negative  $\delta^{13}\text{C}_{\text{carb}}$  excursions as evidence for alteration (see Supplementary Information). However, the observation of a tight coupling between  $\delta^{13}\text{C}_{\text{carb}}$  and  $\delta^{13}\text{C}_{\text{org}}$  through several Neoproterozoic anomalies (Figs 1 and 2) rules out alteration as the primary cause of all large Neoproterozoic negative  $\delta^{13}\text{C}_{\text{carb}}$  excursions (see Supplementary Information). The  $\delta^{18}\text{O}_{\text{carb}}$  in these rocks has almost certainly been reset, given fluid-rock exchange and the high concentration of oxygen in water, but explaining how exchange can reset  $\delta^{13}\text{C}_{\text{carb}}$  given the enormous mass of carbon in carbonate sequences is more challenging<sup>8</sup>. The correlation of  $\delta^{13}\text{C}_{\text{carb}}$  and  $\delta^{18}\text{O}_{\text{carb}}$  is intriguing and may in fact have an environmental/

diagenetic explanation (see Supplementary Information), but requires further investigation. Importantly, however, diagenesis is not responsible for the excursions through which  $\delta^{13}\text{C}$  covaries (Figs 1 and 2).

A complete understanding of the Neoproterozoic carbon cycle requires not only the interpretation of carbon isotope covariance (Figs 1 and 2)<sup>2,4</sup>, but also an explanation for the data that underpinned these alternative hypotheses. We propose that much of the existing  $\delta^{13}\text{C}_{\text{org}}$  from Neoproterozoic sedimentary rocks reflects contamination with a secondary source of organic carbon, possibly from the erosion of organic-rich shale on land or the migration of hydrocarbons within the basin. The isotopic contribution from exogenous sources would be most evident when TOC values are low, consistent with a majority of the published data<sup>10,22</sup>. This hypothesis does not require that all samples with low TOC carry anomalous  $\delta^{13}\text{C}_{\text{org}}$ , but notes the greater susceptibility of these samples<sup>2,4,23</sup> and challenges their universal inclusion in environmental interpretations, especially when  $\delta^{13}\text{C}_{\text{carb}}$  remains constant through intervals when  $\delta^{13}\text{C}_{\text{carb}}$  is variable.

To explore the hypothesis that these data are produced from both an exogenous component and a primary source, we present a model for two-component mixing (Fig. 3a, b). Here, each component carries an organic carbon flux (monitored using TOC) and a distinct  $\delta^{13}\text{C}_{\text{org}}$ , so the product of mixing does not require a linear relationship between components (see Supplementary Information). One component in the model is organic carbon from primary producers (A in Fig. 3a), with a high mass fraction and an isotopic composition offset from dissolved

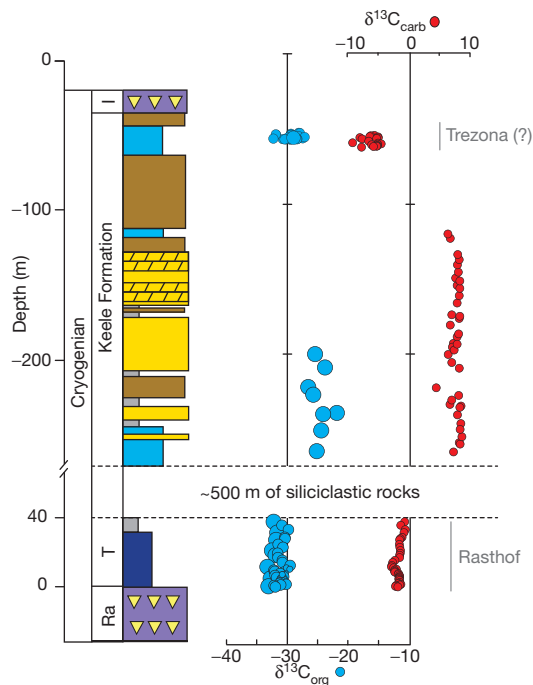


**Figure 2 | A chemostratigraphic section through the late Cryogenian period of northwest Canada.** As in Fig. 1, red circles represent carbonate carbon and blue denotes paired organic carbon ( $n = 73$ ). Isotope scales are equal for carbonate and organic carbon, and the 2-s.d. errors are smaller than the data points. Stratigraphic keys are as in Fig. 1, as are the TOC (wt%) calibrations. Abbreviations correspond to the following: Ra, Rapitan Group; T, Twitya; I, Ice Brook. Carbonate data in the Keele and Twitya formations is from ref. 21 and overall trends are consistent with ref. 4.

inorganic carbon by  $\epsilon_{\text{TOC}}$ . The second component (B in Fig. 3a) is exogenous, and could be terrigenous (detrital) inputs, secondary hydrocarbons, or contamination at some point on the rock's life history (with an isotopic composition in the range of typical organic matter). Post-depositional processes, such as heterotrophic remineralization, will also alter mixed contributions (Fig. 3b). When then compared to  $\delta^{13}\text{C}_{\text{carb}}$  (Fig. 3c, d), this simple mixing model fully describes

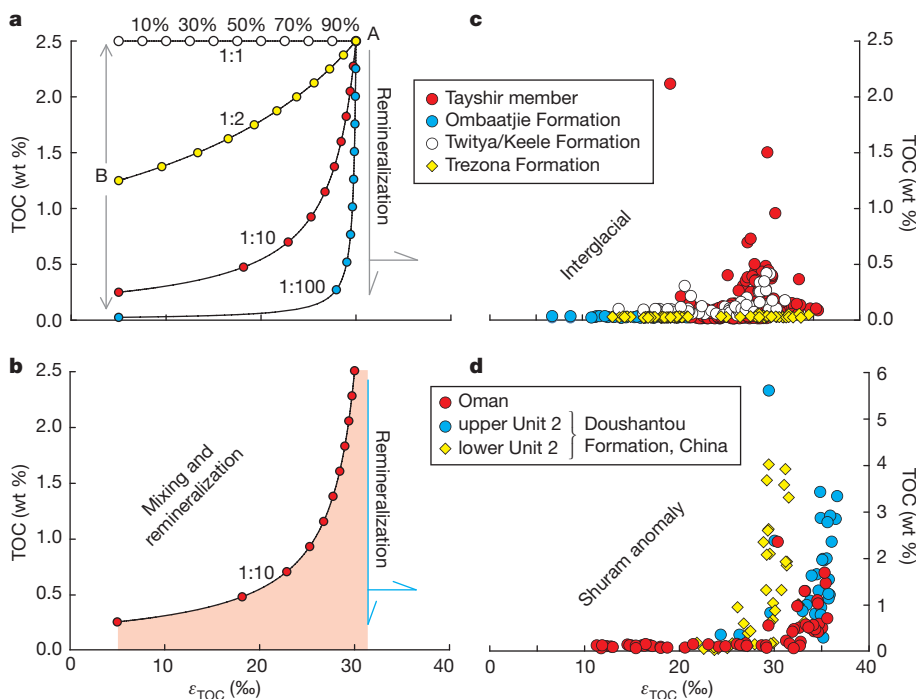


**Figure 3 | A two-component mixing model built to address variability of  $\delta^{13}\text{C}$  with changes in TOC.** Analytical precision for TOC measurements is 0.05 wt % (1 s.d.). **a**, Where the mass fractions of each component are equal, traditional linear mixing is predicted. As one component increases in relative concentration, the mixing array becomes hyperbolic. The ratios listed on the figure denote the relative contribution of A and B. **b**, An example of the zone of possible solutions (red-shaded region) given contributions from a 1:10 mixing, as well as remineralization and post-deposition processes. These processes can alter samples to lower TOC, with modest changes in  $\delta^{13}\text{C}$ . In **c** and **d** the data are binned by age. **c**, Interglacial records from Mongolia and northwest Canada, with additional data from the Ombaatjie Formation (this study; see Supplementary Information;  $n = 79$ ) and Trezona Formation<sup>22</sup>. **d**, Published Shuram data from Oman and China<sup>10,11</sup>. Although the vertical axis is different in **d**, this model approach cleanly explains the excursion.

Cryogenian and Ediacaran records without invoking alteration<sup>7,8</sup> or unfamiliar ocean chemistry<sup>6,10,11,22</sup>. Our model does not require developing and oxidizing an ocean where DOC overwhelms DIC multiple times throughout the Neoproterozoic era, or driving extensive global alteration of carbonate platform sediments. This does not preclude contributions from DOC<sup>24</sup>, but the observation of isotopic covariance at the scales observed requires DOC to be significantly subordinate to DIC<sup>24</sup>. Therefore, we find our model more plausible from a physical and chemical oceanographic standpoint, because it requires only established, well-understood processes (that is, weathering, a circulating ocean and remineralization). It follows from these conclusions that  $\delta^{13}\text{C}_{\text{carb}}$  may be a more faithful indicator of environmental change, and  $\delta^{13}\text{C}_{\text{org}}$  should be viewed critically, especially when TOC is low and invariant.

Given that  $\delta^{13}\text{C}_{\text{carb}}$  may well faithfully preserve primary environmental information, we revisit the reading of this record. The conventional interpretation of the carbon cycle and isotope records uses a simplification of the full carbon flux equation for isotopic mass balance, where  $\delta^{13}\text{C}_{\text{vol}} = [\delta^{13}\text{C}_{\text{org}} \times f_{\text{org}}] + [\delta^{13}\text{C}_{\text{carb}} \times (1 - f_{\text{org}})]$ , and  $f_{\text{org}}$  is the relative fraction of carbon buried as organic matter. In the full carbon flux equation,  $\delta^{13}\text{C}$  inputs reflect a weighted average of volcanism (carbon entrained during subduction and mantle outgassing) and carbonate and organic carbon weathering<sup>25,26</sup>, and the sinks include both carbonate and organic matter burial. So if we consider the full carbon flux equation, other ways of driving  $\delta^{13}\text{C}$  variations become apparent. Each of the above fluxes can change in magnitude and isotopic composition, and each carry specific consequences for climate and oxidant budgets. Also, the Neoproterozoic  $\delta^{13}\text{C}$  excursions occur in tens to hundreds of metres of shallow-water strata (third-order sequence tracts), implying a characteristic timescale of  $10^5$  to  $10^6$  years (ref. 27). It is challenging to produce such large (about 10‰) isotopic excursions, which in certain cases plunge beyond the canonical mantle value, on these timescales without the input of an enormous mass of low- $\delta^{13}\text{C}$  carbon, presumably in the form of either organic matter or methane<sup>28</sup>. This requisite light carbon load may, in part, reflect the mass-balance counterpart to enriched background Cryogenian  $\delta^{13}\text{C}_{\text{carb}}$  values. Such an injection of carbon would also significantly raise atmospheric  $p_{\text{CO}_2}$  or  $p_{\text{CH}_4}$  and consume existing oxidant reservoirs<sup>29</sup>, which is difficult to reconcile with the close stratigraphic association of at least some of the excursions and glacial deposits<sup>26</sup>. Another possibility is that

the oxidation of reduced carbon is accomplished with  $\text{SO}_4^{2-}$  or Fe oxides as the electron acceptor<sup>30</sup>, rather than  $\text{O}_2$ , which may allow for some stabilization of  $p_{\text{CO}_2}$  through the effect on alkalinity<sup>24</sup>. If the duration of these events is found to be longer, then carbon mass input arguments should be modified accordingly, but the relevant reservoirs interacting with the surface carbon cycle remain unchanged.

The data and analysis presented here illustrates that  $\delta^{13}\text{C}_{\text{carb}}$  preserves a faithful snapshot of the Neoproterozoic surface carbon cycle. This suggests that there is an environmental explanation for the enriched  $\delta^{13}\text{C}_{\text{carb}}$  background values, and that at least some of the  $10^5$ -to- $10^6$ -year negative  $\delta^{13}\text{C}_{\text{carb}}$  excursions reflect primary features of the surface carbon cycle. These anomalies thus require the episodic input of isotopically light carbon, presumably methane or organic matter, as well as the cyclic consumption and production of electron acceptors such as sulphate and  $\text{O}_2$ . Our data do not eliminate diagenetic explanations for particular excursions throughout the world, but the covariation evident during many of the excursions does suggest a common explanation for all of them. Whether these excursions are driven by the recycling of stored carbon in the form of methane hydrate or ancient organic matter in sediments, or by the dynamics of nutrient-dependent productivity in the ocean remains uncertain. Consistent with both is the idea is that these excursions simply reflect a series of failed transitions from the more reducing and biologically simple Proterozoic world towards the more oxidizing and biologically complex Phanerozoic Earth on which we now live.

## METHODS SUMMARY

All isotope data are presented relative to the Vienna PeeDee Belemnite (VPDB) standard and calculated according to standard delta notation and reported in units of ‰. Carbonate carbon and oxygen isotope measurements were made as one individual measurement, with the organic carbon isotopic composition measured separately, but on the same hand sample. Carbonate carbon isotopes were prepared by cutting hand samples to expose a fresh surface followed by micro-drilling 0.001 g. A small aliquot of this powder was analysed on a VG Optima run in dual inlet mode, abutted to a common acid bath preparation device. Samples were acidified in  $\text{H}_3\text{PO}_4$  at 90 °C. The evolved  $\text{CO}_2$  was cryo-focused and analysed against an in-house standard reference gas. The reproducibility of this measurement was better than 0.1‰ (one standard deviation). Organic carbon analyses were performed on large (about 10 g) samples to accommodate low TOC values. Samples were decalcified with concentrated HCl for 48 h, buffered back to a neutral pH (>pH 5), filtered and dried. The mass of insoluble residue was taken as siliciclastic content. Homogenized residues were analysed on a Carlo Erba Elemental Analyzer attached to a ThermoFinnigan Delta V configured in continuous flow mode. Samples and standards were bracketed such that our >350 unique organic carbon analyses (each run in duplicate) were associated with 370 internal standards. These standards have known organic carbon contents and isotope values, and were used to calibrate TOC contents and isotopic compositions. Estimates of error are also reported in the text. The simple mixing model underpinning Fig. 3 is a standard multi-component mixing scenario.

**Full Methods** and any associated references are available in the online version of the paper at [www.nature.com/nature](http://www.nature.com/nature).

Received 28 June 2011; accepted 9 January 2012.

Published online 29 February 2012.

- Halverson, G. P., Wade, B. P., Hurtgen, M. T. & Barovich, K. M. Neoproterozoic chemostratigraphy. *Precamb. Res.* **182**, 337–350 (2010).
- Knoll, A. H., Hayes, J. M., Kaufman, A. J., Swett, K. & Lambert, I. B. Secular variation in carbon isotope ratios from upper Proterozoic successions of Svalbard and east Greenland. *Nature* **321**, 832–838 (1986).
- Des Marais, D. J., Strauss, H., Summons, R. E. & Hayes, J. M. Carbon isotope evidence for the stepwise oxidation of the Proterozoic environment. *Nature* **359**, 605–609 (1992).
- Kaufman, A. J., Knoll, A. H. & Narbonne, G. M. Isotopes, ice ages, and terminal Proterozoic earth history. *Proc. Natl Acad. Sci. USA* **94**, 6600–6605 (1997).
- Hayes, J. M., Strauss, H. & Kaufman, A. J. The abundance of C-13 in marine organic matter and isotopic fractionation in the global biogeochemical cycle of carbon during the past 800 Ma. *Chem. Geol.* **161**, 103–125 (1999).
- Rothman, D. H., Hayes, J. M. & Summons, R. E. Dynamics of the Neoproterozoic carbon cycle. *Proc. Natl Acad. Sci. USA* **100**, 8124–8129 (2003).

- Knauth, L. P. & Kennedy, M. J. The late Precambrian greening of the Earth. *Nature* **460**, 728–732 (2009).
- Derry, L. A. A burial diagenesis origin for the Ediacaran Shuram-Wonoka carbon isotope anomaly. *Earth Planet. Sci. Lett.* **294**, 152–162 (2010).
- Canfield, D. E., Poulton, S. W. & Narbonne, G. M. Late-Neoproterozoic deep-ocean oxygenation and the rise of animal life. *Science* **315**, 92–95 (2007).
- Fike, D. A., Grotzinger, J. P., Pratt, L. M. & Summons, R. E. Oxidation of the Ediacaran Ocean. *Nature* **444**, 744–747 (2006).
- McFadden, K. A. *et al.* Pulsed oxidation and biological evolution in the Ediacaran Doushantuo Formation. *Proc. Natl Acad. Sci. USA* **105**, 3197–3202 (2008).
- Grotzinger, J. P., Fike, D. A. & Fischer, W. W. Enigmatic origin of the largest-known carbon isotope excursion in Earth's history. *Nature Geosci.* **4**, 285–292 (2011).
- Macdonald, F. A., Jones, D. S. & Schrag, D. P. Stratigraphic and tectonic implications of a new glacial diamicrite-cap carbonate couplet in southwestern Mongolia. *Geology* **37**, 123–126 (2009).
- Halverson, G. P., Hoffman, P. F., Schrag, D. P., Maloof, A. C. & Rice, A. H. N. Toward a Neoproterozoic composite carbon-isotope record. *Geol. Soc. Am. Bull.* **117**, 1181–1207 (2005).
- McCay, G. A., Prave, A. R., Alsop, G. I. & Fallick, A. E. Glacial trinity: Neoproterozoic Earth history within the British-Irish Caledonides. *Geology* **34**, 909–912 (2006).
- McKirdy, D. M. *et al.* A chemostratigraphic overview of the late Cryogenian interglacial sequence in the Adelaide fold-thrust belt, South Australia. *Precamb. Res.* **106**, 149–186 (2001).
- Halverson, G. P., Hoffman, P. F., Schrag, D. P. & Kaufman, A. J. A major perturbation of the carbon cycle before the Ghaub glaciation (Neoproterozoic) in Namibia: prelude to snowball Earth? *Geochim. Geophys. Geosyst.* **3**, 1035, <http://dx.doi.org/10.1029/2001GC000244> (2002).
- Hoffman, P. F., Kaufman, A. J., Halverson, G. P. & Schrag, D. P. A Neoproterozoic snowball earth. *Science* **281**, 1342–1346 (1998).
- Hoffmann, K. H., Condon, D. J., Bowring, S. A. & Crowley, J. L. U-Pb zircon date from the Neoproterozoic Ghaub Formation, Namibia: constraints on Marinoan glaciation. *Geology* **32**, 817–820 (2004).
- Macdonald, F. A. *et al.* Calibrating the Cryogenian. *Science* **327**, 1241–1243 (2010).
- Hoffman, P. F. & Schrag, D. P. The snowball Earth hypothesis: testing the limits of global change. *Terra Nova* **14**, 129–155 (2002).
- Swanson-Hyssel, N. L. *et al.* Cryogenian glaciation and the onset of carbon-isotope decoupling. *Science* **328**, 608–611 (2010).
- Dehler, C. M. *et al.* High-resolution delta C-13 stratigraphy of the Chuar Group (ca. 770–742 Ma), Grand Canyon: implications for mid-Neoproterozoic climate change. *Geol. Soc. Am. Bull.* **117**, 32–45 (2005).
- Tziperman, E., Halevy, I., Johnston, D. T., Knoll, A. H. & Schrag, D. P. Biologically induced Snowball Earth. *Proc. Natl Acad. Sci.* **108** (37), 15091–15096 (2011).
- Hayes, J. M. & Waldbauer, J. R. The carbon cycle and associated redox processes through time. *Phil. Trans. R. Soc. B* **361**, 931–950 (2006).
- Schrag, D. P., Berner, R. A., Hoffman, P. F. & Halverson, G. P. On the initiation of a snowball Earth. *Geochim. Geophys. Geosyst.* **3**, 1036, <http://dx.doi.org/10.1029/2001gc000219> (2002).
- Halverson, G. P., Hoffman, P. F., Schrag, D. P. & Kaufman, A. J. A major perturbation of the carbon cycle before the Ghaub glaciation (Neoproterozoic) in Namibia: prelude to snowball Earth? *Geochim. Geophys. Geosyst.* **3**, 1035, <http://dx.doi.org/10.1029/2001gc000244> (2002).
- Bjerrum, C. J. & Canfield, D. E. Towards a quantitative understanding of the late Neoproterozoic carbon cycle. *Proc. Natl Acad. Sci. USA* **108**, 5542–5547 (2011).
- Bristow, T. F. & Kennedy, M. J. Carbon isotope excursions and the oxidant budget of the Ediacaran atmosphere and ocean. *Geology* **36**, 863–866 (2008).
- Johnston, D. T. *et al.* An emerging picture of Neoproterozoic ocean chemistry: Insights from the Chuar Group, Grand Canyon, USA. *Earth Planet. Sci. Lett.* **290**, 64–73 (2010).
- Levashova, N. M. *et al.* The origin of the Baydaric microcontinent, Mongolia: constraints from paleomagnetism and geochronology. *Tectonophysics* **485**, 306–320 (2010).

**Supplementary Information** is linked to the online version of the paper at [www.nature.com/nature](http://www.nature.com/nature).

**Acknowledgements** Laboratory assistance was provided by G. Eischeid, E. Northrop, E. Kennedy, T. O'Brien, A. Breus and A. Masterson. We thank G. Halverson, A. Bradley, E. Tziperman and P. Huybers for discussions and comments. We thank the Yukon Geological Survey, the NSF (grant number EAR-IF 0949227 to D.T.J.), KINSC (Haverford College), Henry and Wendy Breck (to D.P.S.), ESEP (Canadian Institute for Advanced Research, to P.F.H.), Harvard University and NASA NAI (D.T.J. and F.A.M.) for funding.

**Author Contributions** This project was conceived by D.T.J., F.A.M. and D.P.S. Field work was conducted by F.A.M. and P.F.H. Carbonate carbon analyses were performed by F.A.M. Organic carbon analyses and modelling were carried out by D.T.J. and B.C.G. The paper was written by all authors.

**Author Information** Reprints and permissions information is available at [www.nature.com/reprints](http://www.nature.com/reprints). The authors declare no competing financial interests. Readers are welcome to comment on the online version of this article at [www.nature.com/nature](http://www.nature.com/nature). Correspondence and requests for materials should be addressed to D.T.J. ([johnston@eps.harvard.edu](mailto:johnston@eps.harvard.edu)).

## METHODS

All isotope data are presented relative to the Vienna PeeDee Belemnite (VPDB) standard and calculated according to standard delta notation and reported in units of ‰. Carbonate carbon and oxygen isotope measurements made as one individual measurement, with the organic carbon isotopic composition measured separately, but on the same hand sample. Carbonate carbon isotopes were prepared by cutting hand samples to expose a fresh surface followed by micro-drilling 0.01 g. A small aliquot of this powder was analysed on a VG Optima run in dual inlet mode, abutted to a common acid bath preparation device. Samples were acidified in H<sub>3</sub>PO<sub>4</sub> at 90 °C. The evolved CO<sub>2</sub> was cyro-focused and analysed against an in-house standard reference gas. The reproducibility of this measurement was better than 0.1‰ (one standard deviation). Organic carbon analyses were performed on large (about 10 g) samples to accommodate low TOC values. Samples were decalcified with concentrated HCl for 48 h, buffered back to a neutral pH (>pH 5), filtered, and dried. The mass of insoluble residue was taken as siliciclastic content. Homogenized residues were analysed on a Carlo Erba Elemental Analyzer attached to a ThermoFinnigan Delta V configured in continuous flow mode. Samples and standards were bracketed such that our >350 unique organic carbon analyses (each run in duplicate) were associated with 370

internal standards. These standards have known organic carbon contents and isotope values, and were used to calibrate TOC contents and isotopic compositions. Estimates of error are reported in the text.

The model presented in the manuscript is a multi-component mixing scenario, herein defined by a hyperbolic relationship. The equation represents a style of two-component mixing, where:

$$(\delta^{13}\text{C}_{\text{TOC}})_M = (\delta^{13}\text{C}_{\text{TOC}})_A \times f_A \times (X_A/X_M) + (\delta^{13}\text{C}_{\text{TOC}})_B \times (1 - f_A)(X_B/X_M)$$

with the subscripts M, A and B representing the mixture, end-member A and end-member B. There are two weighting factors  $f_A$  and  $(1 - f_A)$ , which are fractional terms seen in the equation describing linear mixing:

$$X_M = X_A \times f_A + X_B \times (1 - f_A)$$

where  $X$  is mass. In solving this, we can choose the end-member compositions— $X_A$ ,  $(\delta^{13}\text{C}_{\text{TOC}})_A$ ,  $X_B$  and  $(\delta^{13}\text{C}_{\text{TOC}})_B$ —and allow  $f_A$  to vary from 0 to 1 (this is a relative flux term). This allows us to solve for  $X_M$  (from equation (2)) and then  $(\delta^{13}\text{C}_{\text{TOC}})_M$  from equation (1)). For application in Fig. 3, we can include the  $\delta^{13}\text{C}_{\text{carb}}$  on the same sample.